

INTERSTELLAR SCINTILLATION OF PULSAR RADIATION*

KENNETH R. LANG

Cornell-Sydney University Astronomy Center, Arecibo Observatory

Received 1970 July 27; revised 1970 October 8

ABSTRACT

It is demonstrated that the long-term fluctuations in the intensity of pulsar radiation are due to interstellar scintillation. Observed statistical quantities are consistent with a thin-screen model in which the screen is located halfway between the Earth and the pulsar. Decorrelation frequencies are found to be proportional to the fourth power of the observing frequency and inversely proportional to the square of the dispersion measure. Power spectra are nearly Gaussian in form, but have a high-frequency tail which may be power law. Observed pulse broadening is shown to be equivalent to the convolution of the emitted pulse profile with an exponential function for which the e^{-1} decay time is the reciprocal of the decorrelation frequency. Decorrelation times are found to be proportional to the observing frequency and weakly dependent on dispersion measure. Modulation indices are nearly unity and independent of observing frequency in the interval 111–606 MHz. Both Rice-squared and lognormal probability distribution functions fit the observed probability distributions of intensity well. The scale size is $\approx 10^{11}$ cm, roughly the size of the first Fresnel zone, and the rms fluctuating number density of electrons is 3×10^{-4} cm $^{-3}$. The scattering becomes weak above 2000 MHz for nearby pulsars. These scintillation measurements provide estimates for pulsar distances which, when used with known dispersion measures, indicate that the average number density of electrons along the line of sight to the pulsars is 0.03 cm $^{-3}$. Pulsars must be smaller than 10^{-7} seconds of arc in order to give rise to the observed intensity fluctuations. This size is considerably below the angular size of any observable self-absorbed synchrotron radio source. The relative velocities of the pulsar and/or the interstellar medium with respect to the Earth lie in the range 30–200 km sec $^{-1}$. Pulsars with periods smaller than a few milliseconds will not be detected at frequencies below a few hundred MHz. The minimum detectable angular size of a radio source at a distance of 300 pc is on the order of 10^{-3} seconds of arc at 318 MHz. This limiting size is proportional to the square root of the distance and inversely proportional to the square of the observing frequency. The view that the compact source in the Crab Nebula is the pulsar NP 0532 which has been broadened by interstellar scattering is consistent with these measurements.

I. INTRODUCTION

The time variations of the intensity of pulsar radiation may be described by the superposition of short-term fluctuations with time scales of seconds and long-term fluctuations with time scales of several minutes. Scheuer (1968) has shown that the short-term fluctuations are most probably intrinsic to the source, and both Scheuer (1968) and Salpeter (1969) have suggested that the long-term fluctuations may be scintillations caused by irregularities in the interstellar medium. Rickett (1969) has provided some evidence for the interstellar-scintillation hypothesis by observing a correlation between dispersion measure and the characteristic bandwidth over which the intensity variations are correlated. Additional evidence has been provided by Lang (1969), who has shown that many of the observed statistical quantities are consistent with the predictions of the theory of thin-screen scintillation. Recent observations of highly correlated intensity fluctuations over a 6400-km baseline with time delays on the order of seconds (Lang and Rickett 1970) have further substantiated that the observed variations in the intensity of pulsar radiation are due to interstellar scintillation.

In this paper we provide a comprehensive set of various statistical quantities obtained from digital recordings of the power detected while observing pulsars. Those readers who are primarily interested in these observations and the subsequent deductions concerning

* Portions of this paper were presented at the Fourteenth General Assembly of the I A U and at the Accademia Nazionale Dei Lincei meeting on pulsars and high-energy activity in supernova remnants.

pulsars and the interstellar medium will find it convenient to read §§ III, IV, and V. In order to provide functional relationships which may be compared with the observations, however, we present in § II of this paper a short summary of the theory of thin-screen scintillation. A model is selected in which a thin phase-changing screen is located halfway between the Earth and the pulsar. Dispersion measure is introduced as a theoretical parameter by assuming that the effective screen thickness is the distance between the pulsar and the Earth and that the fluctuating electron number density is proportional to the electron number density. A detailed comparison of observed statistical quantities with the theoretical model is carried out in § III. It is shown that, under the previous assumptions, observations of decorrelation frequencies, pulse broadening, decorrelation times, modulation indices, scale sizes, and critical frequencies are all consistent with the thin-screen model. In § IV, the measurements given in § III are used to provide estimates for pulsar distances, the average number density of electrons along the line of sight to the pulsars, the angular sizes of pulsars, relative velocities of the pulsar and/or the interstellar medium with respect to the Earth, the minimum detectable period of a pulsar, and the minimum detectable size of a radio source.

II. THEORY OF THIN-SCREEN SCATTERING

Although interstellar scattering is probably caused by a somewhat thick distribution of plasma turbules, no complete theory yet exists for interstellar scintillation where both the pulsar and the observer are immersed in an extended medium. One approximate approach would be to assume that the pulsar is located at an infinite distance, and that the scattering is caused by an extended medium (cf. Fejer 1953; Uscinski 1968*a, b*). A much simpler approach, however, is to assume that the scattering has been produced by a thin phase-changing screen located midway between the pulsar and the Earth. This thin-screen model will certainly give correct order-of-magnitude estimates of the relevant characteristic parameters. In fact, the estimates obtained by using the thin-screen model (cf. §§ III and IV) closely parallel those obtained by the more complicated extended-medium analysis (Rickett 1970).

The theory of scattering in this thin-phase-screen approximation has been reviewed and extended by Salpeter (1967), and here we will adopt simple explanations for the relevant formulae. Let us assume that interstellar scattering is caused by a collection of plasma turbules distributed uniformly in space. When a plane wave of frequency ν passes through a turbule of size a , the phase change $\Delta\phi$ caused by a fluctuation in the plasma electron density is $\Delta\phi = r_e \Delta n_e a c / \nu$, where $r_e = 2.82 \times 10^{-13}$ cm and is the classical electron radius, Δn_e is the fluctuating electron number density, and c is the velocity of light. Small random variations in the electron density may be taken to be statistically homogeneous and stationary with respect to spatial coordinates, and to have a Gaussian autocorrelation function whose variance is a . The pulsar is taken to be located at a distance D along the line of sight between the Earth and the pulsar, and the plasma turbules are assumed to be isotropically distributed in the galactic disk. Under these conditions, the phase fluctuations are characterized by the rms value, ϕ_0 , given by

$$\phi_0 = (D/a)^{1/2} \langle \Delta\phi^2 \rangle^{1/2} \approx 8.5 \times 10^{-3} \nu^{-1} (Da)^{1/2} \langle \Delta n_e^2 \rangle^{1/2}, \quad (1)$$

where the angular brackets denote a spatial average.

The scattering will be taken to be equivalent to that of a thin screen located midway between the pulsar and the Earth. If geometric optics is used, a normally incident plane wave will be scattered by the thin screen into the rms scattering angle θ_{scat} , given by

$$\theta_{\text{scat}} = \left(\frac{\phi_0 c}{2\pi a \nu} \right) \approx 4 \times 10^7 \left(\frac{D}{a} \right)^{1/2} \frac{\langle \Delta n_e^2 \rangle^{1/2}}{\nu^2}. \quad (2)$$

It is noted that θ_{scat} may be the minimum detectable size of a radio source, and that measurements of θ_{scat} at low radio frequencies may provide measurements of $(D\langle\Delta n_e^2\rangle)^{1/2}$.

The path difference between scattered and direct rays will be $\frac{1}{4}D(\theta_{\text{scat}})^2$. If signals are observed over bandwidths larger than $4cD^{-1}(\theta_{\text{scat}})^{-2}$, the diffraction patterns from different observed frequencies will interfere. Consequently, fluctuations in the intensity of pulsar radiation will be observed only when the bandwidths are smaller than the decorrelation frequency,

$$f_\nu = \frac{4c}{D(\theta_{\text{scat}})^2} \approx \frac{7 \times 10^{-5} a \nu^4}{\langle\Delta n_e^2\rangle D^2}. \quad (3)$$

Once a and $\langle\Delta n_e^2\rangle^{1/2}$ are known, measurements of decorrelation frequency may be used to provide estimates of pulsar distances. These estimates may then be used with the dispersion measures to obtain the average electron density, $\langle n_e \rangle$, along the line of sight to the pulsar.

In order to compare observable parameters with a measurable pulsar parameter, it is convenient to assume that $\langle\Delta n_e^2\rangle^{1/2}$ is proportional to $\langle n_e \rangle$. In this case

$$f_\nu \propto \frac{\nu^4}{(\int n_e dl)^2}, \quad (4)$$

where $\int n_e dl$ is the dispersion measure of the pulsar.

Assuming that the variations in electron density have a Gaussian autocorrelation function, Fejer (1953) has shown that the flux scattered from a thin screen has a Gaussian distribution in θ , with an rms value of θ_{scat} . The scattered radiation is delayed in time relative to the unscattered radiation by $\frac{1}{4}D\theta^2/c$, and consequently an infinitely sharp pulse of radiation will be scattered into a pulse whose time profile will be an exponential function whose e^{-1} decay time is f_ν^{-1} . As Cronyn (1970a) has pointed out, observed pulsar profiles will be the convolution of the emitted profiles with this exponential. Therefore, measurements of f_ν will also provide a measure of the minimum detectable pulsar period.

The scale of the diffraction pattern at the Earth will be $c/\nu\theta_{\text{scat}}$. The pattern from different point sources whose spacing is larger than $c/\nu D\theta_{\text{scat}}$ will interfere, and will result in a smeared diffraction pattern. Consequently, radio sources larger than the critical angle

$$\psi_c = \frac{c}{\nu D\theta_{\text{scat}}} \approx 10^3 \left(\frac{a}{D}\right)^{1/2} \frac{\nu}{D\langle\Delta n_e^2\rangle^{1/2}} \quad (5)$$

will give rise to very weak fluctuations in intensity. In fact, observed fluctuations in the intensity of pulsar radiation are strong, and the pulsars must be smaller than ψ_c .

If the plasma turbules move at a velocity v transverse to the line of sight to the pulsar, the observed intensity of pulsar radiation will fluctuate with a time scale on the order of $c/\nu v\theta_{\text{scat}}$. Therefore, a decorrelation time is defined as

$$\tau_\nu = \frac{c}{\nu v\theta_{\text{scat}}} \approx 10^3 \left(\frac{a}{D}\right)^{1/2} \frac{\nu}{v\langle\Delta n_e^2\rangle^{1/2}} \propto \frac{\nu}{(\int n_e^2 dl)^{1/2}}. \quad (6)$$

Measurements of decorrelation times may be used to provide estimates of v .

Because the observed fluctuations in the intensity of pulsar radiation are deep, the number of high-intensity pulses will be greater than that expected from a Gaussian distribution of intensities. In fact, Mercier (1962) has shown that the probability distribution $P(I)$ of observed intensities I will be Rice-squared, and Cohen *et al.* (1967) have given mathematical expressions which relate $P(I)$ to the average intensity and the modulation index. The modulation index is the relative rms value of the intensity fluctuations about the mean intensity, and is expected to be nearly unity at all radio

frequencies for which deep fluctuations in intensity are prevalent. For large phase deviations, $\phi_0 \gg 1$, the Rice-squared intensity distribution will become an exponential function of intensity.

Deep intensity fluctuations will continue to be prevalent as long as several cones of scattered radiation are observed at the same time, and as long as the rms phase deviation ϕ_0 is greater than one—that is, as long as

$$\frac{2a}{D} < \theta_{\text{scat}} \quad \text{and} \quad a > \frac{c}{2\pi\nu\theta_{\text{scat}}} = \frac{a}{\phi_0}. \quad (7)$$

The correlation length of the electron-density fluctuations a may be directly determined from the parameters of equation (7).

Equations (2) and (7) define a critical frequency ν_c above which interstellar scattering will become weak:

$$\nu_c^2 \approx 2 \times 10^7 (D/a)^{3/2} \langle \Delta n_e^2 \rangle^{1/2}. \quad (8)$$

This high-frequency range is characterized by a decorrelation time which is independent of frequency, small modulation indices, and a nearly Gaussian distribution of intensities.

III. OBSERVATIONS

a) Observing Techniques

Linearly polarized antennas were used at 195, 318, and 606 MHz, and circularly polarized antennas were used at 111 and 430 MHz. In all cases, the power detected by radiometers was sampled digitally at the rate specified by the RC time constant and the sampling theorem. Pulsar periods were calculated for each observation by using the known rate of period change intrinsic to each pulsar and the known rate of motion of the Earth with respect to the Sun. These periods were accurate to 1 microsecond. When intensities were required, pulse intensities (ON intensities) were calculated by integrating the power within windows of data which were slightly wider than one pulse width and which were centered on each pulse. Similarly, intensities due to system noise (OFF intensities) were calculated for windows placed midway between pulses.

b) Decorrelation Frequencies

Observations by Scott and Collins (1968) at 80 MHz and by Komesaroff *et al.* (1968) at 150 MHz first indicated that pulsar radiation contains fine frequency structure. Measurements of the decorrelation bandwidth B_H made by Rickett (1969) at 408 MHz showed that $B_H \approx 0.3 f_{408}$ was proportional to the inverse square of dispersion measure, indicating that those electrons which are responsible for the dispersion are also responsible for the frequency structure.

Although Rickett's observed correlation between B_H and dispersion measure is predicted by equation (4), Huguenin, Taylor, and Jura (1969) have found the apparent widths of average spectral features scale as ν^2 , and not as the ν^4 predicted by equation (4). Their measurement of $f_{234} = 0.2$ MHz for CP 0328, however, disagrees with recent measurements by Ewing *et al.* (1970), who find that CP 0328 has $f_{234} \approx 10$ kHz and $f_{168} < 2$ kHz.

In order to examine further the frequency dependence of decorrelation frequency, several pulsars have been observed at 111 and 318 MHz with the Arecibo antenna. Pulse intensities were calculated from data which were simultaneously recorded with five radiometers which had 10-msec time constants and contiguous 10-, 25-, 100-, or 500-kHz bandwidths. Cross-correlation coefficients, $\Gamma_{12}(0)$, were determined by taking cross-correlations between sequences of intensity which were between 2048 and 8192 points long. The cross-correlation function $\Gamma_{12}(\tau)$ of the intensities $I_1(t)$ and $I_2(t)$ recorded at time t by radiometers 1 and 2 is defined as

$$\Gamma_{12}(\tau) = \frac{1}{\sigma_1\sigma_2} \left\langle [I_1(t) - \langle I_1(t) \rangle][I_2(t + \tau) - \langle I_2(t + \tau) \rangle] \right\rangle, \quad (9)$$

where the angular brackets denote a time average and σ_1^2 and σ_2^2 are the mean square deviations of $I_1(t)$ and $I_2(t)$, respectively.

The frequency correlation function was then formed by plotting $\Gamma_{12}(0)$ versus the separation of the radiometer radio frequencies (Figs. 1 and 2). The error bars denote the rms fluctuations of the cross-correlation function $\Gamma_{12}(\tau)$ for nonzero lags.

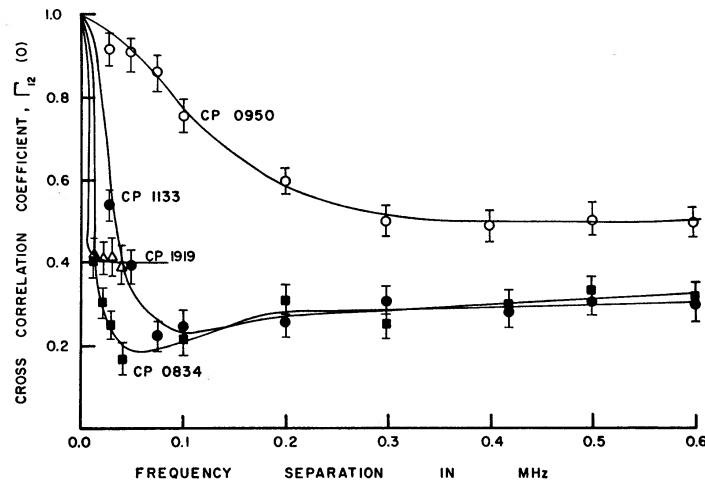


FIG. 1.—Cross-correlation coefficients, $\Gamma_{12}(0)$, formed from cross-correlations of sequences of intensities between 2048 and 8192 points long. The intensities were taken from data simultaneously recorded by radiometers with 10-msec time constants, contiguous 10-, 25-, or 100-kHz bandwidths, and radio frequencies near 111 MHz. The abscissa denotes the separation of the radio frequencies, and the error bars denote the rms fluctuations of the cross-correlation function for nonzero lags.

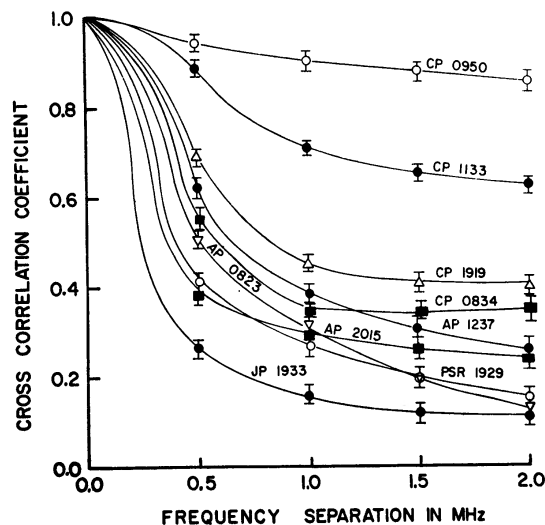


FIG. 2.—Cross-correlation coefficients, $\Gamma_{12}(0)$, formed from cross-correlations of sequences of intensities between 2048 and 8192 points long. The intensities were taken from data simultaneously recorded by radiometers with 10-msec time constants, contiguous 500-kHz bandwidths, and radio frequencies near 318 MHz. The abscissa denotes the separation of the radio frequencies, and the error bars denote the rms fluctuations of the cross-correlation function for nonzero lags.

Because $\Gamma_{12}(0)$ may be as large as 0.4 for frequency differences as large as several hundred MHz (cf. Lang 1969), the decorrelation frequency f_ν is defined as that frequency separation for which the cross-correlation coefficient becomes half of one minus its value at very high-frequency separations. A plot of f_{111} and f_{318} versus dispersion measure is shown in Figure 3, together with the $f_{408} \approx 0.3 B_H$ measured by Rickett (1969). The three lines in this figure denote a decorrelation frequency which is proportional to the fourth power of observing frequency and inversely proportional to the square of the dispersion measure. These measurements indicate that f_ν is proportional to $(\int n_e dl)^{-2} \nu^{4.0 \pm 0.3}$. These results agree with equation (4) and are in agreement with other measurements by Komesaroff *et al.* (1968), Rickett (1970), and Ewing *et al.* (1970). A summary of these various measurements of f_ν is given in Table 1, together with values for other parameters of the interstellar scattering medium.

It should be stressed here that measurements of narrow band structure at low radio frequencies are in agreement with basic scintillation theory. However, this does not necessarily imply that there may not be other, larger frequency structures which may or may not be related to scintillation. In fact, frequency structure which has a width that varies as the cube of frequency and has a value of a few hundred kHz at 100 MHz will result from Faraday rotation in the interstellar medium (cf. Staelin and Reifenstein 1969; Vitkevich and Shitov 1970).

c) Pulse Broadening

The superposition of pulsar flux arriving along direct and scattered paths will cause an emitted pulse to be asymmetrically broadened in time by an amount which is proportional to the square of the scattering angle. Fejer (1953) has pointed out that the distribution function for the angular scattering can be taken to be Gaussian with the rms value, θ_{scat} . As Cronyn (1970a) has shown, it follows that the profile of the observed pulses will be

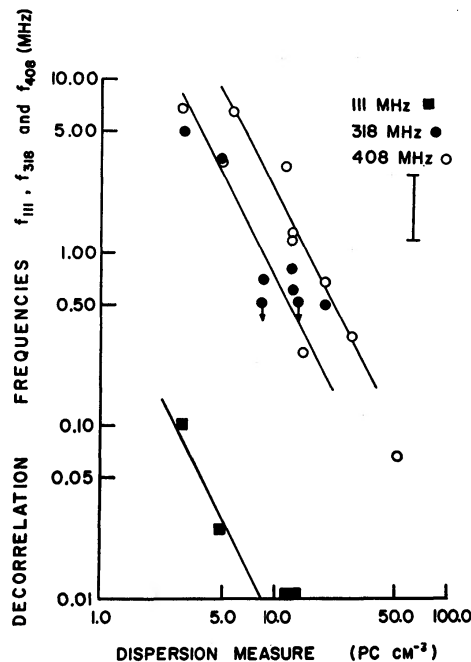


FIG. 3.—Decorrelation frequencies at 111, 318, and 408 MHz. Solid lines denote decorrelation frequencies which are proportional to the fourth power of observing frequency and inversely proportional to the square of the dispersion measure. The 408-MHz data are taken from Rickett (1969) with $f_{408} \approx 0.3 B_{408}$.

TABLE 1
INTERSTELLAR-SCINTILLATION PARAMETERS FOR PULSARS*

Pulsar	f_{218} (MHz)	f_{408} (MHz)	τ_{218} (10^3 sec)	D (pc)	$\int n_e dl$ (pc cm $^{-3}$)	$\langle n_e \rangle$ (cm $^{-3}$)
CP 0328.....	...	0.3	...	755	26.7	0.035
NP 0532.....	0.013†	2220	56.81	0.026
CP 0808.....	...	6.7	...	160	5.8	0.036
AP 0823.....	0.5	...	1.1	354	19.47	0.055
CP 0834.....	0.5	1.3	1.0	362	12.86	0.035
CP 0950.....	>2.0	6.7	3.2	160	2.97	0.018
CP 1133.....	2.0	3.3	1.3	150	4.85	0.032
AP 1237.....	0.7	...	0.8	300	9.29	0.031
HP 1506.....	...	0.7	...	494	19.6	0.039
PSR 1749.....	...	0.07	...	1563	50.9	0.033
CP 1919.....	0.8	1.2	1.1	377	12.43	0.033
JP 1933.....	0.001†	7900	158.60	0.020
AP 2015.....	<0.5	0.3	...	755	14.18	0.018
PSR 2045.....	...	3.3	...	228	11.4	0.050

* $f_{408} = 0.3B_{408}$, where B_{408} is from Rickett (1969), D is from equation (4) with $a = 10^{11}$ cm and $(\Delta n_e^2)^{1/2} = 3 \times 10^{-4}$ cm $^{-3}$, and the $\int n_e dl$ are from Craft (1970) and Rickett (1969).

† From the pulse broadening at 111 MHz and equation (3).

the convolution of the emitted pulses with an exponential function whose e^{-1} decay time is f_ν^{-1} . If one uses equation (4) and assumes that the respective $\int n_e dl$ for CP 1133 and NP 0532 are 4.85 and 56.81 pc cm $^{-3}$ and that $f_{408} = 3 \times 10^6$ Hz for CP 1133, it follows that $f_{111}^{-1} \approx 10$ msec for NP 0532. Both Staelin and Sutton (1970) and Rankin *et al.* (1970) have shown that $f_{111}^{-1} \approx 10$ msec for NP 0532, if it is assumed that the emitted pulse width is not a strong function of frequency. They also show that f_ν^{-1} is proportional to $\nu^{-4 \pm 1}$ for this pulsar. Staelin *et al.* observe exponential pulse shapes for strong single pulses at 115 and 157 MHz. Rankin *et al.*, however, have compared average pulse profiles of NP 0532 with theoretical profiles generated from exponential, Rayleigh, and Gaussian functions. None of these simple functions describe all of their observed profiles well, but the function $\tau \exp(-\tau)$, where τ is the time variable, fits the set of observations best. Such a comparison is confused, however, by the four component pulses whose polarization and radio spectra probably differ. In addition, the average pulse profiles are probably affected by refraction effects in the supernova shell.

In order to examine pulse broadening further, the average pulse profiles of the pulsar JP 1933 have been obtained (Figs. 4 and 5). In each case, digital data were obtained from radiometers whose bandwidth was 10 kHz and whose integration time τ_0 is denoted in Figures 4 and 5. The average profile was then calculated by adding samples which were spaced by an integral number of pulsar periods. The observed profiles indicate a progressive broadening at the lower radio frequencies, and confirm Craft's (1970) observation that the 430- and 195-MHz pulse widths differ by a factor of 2.

It is especially interesting to compare the f_{111}^{-1} for JP 1933 with that of NP 0532. When we note that $f_{111}^{-1} \approx 10$ msec for NP 0532 and that $\int n_e dl = 56.81$ and 158.60 pc cm $^{-3}$ for NP 0532 and JP 1933, respectively, the assumption that f_ν^{-1} is proportional to the square of dispersion measure leads us to conclude that $f_{111}^{-1} \approx 78$ msec for JP 1933. As this is the observed value for JP 1933 (cf. Fig. 5), the two results indicate that the pulse broadening is proportional to the square of dispersion measure. Such a comparison is possible only for these more distant pulsars, where the broadening due to interstellar scintillation is substantially larger than the emitted pulse width.

The instrumental-broadening function caused by postdetection integration and disper-

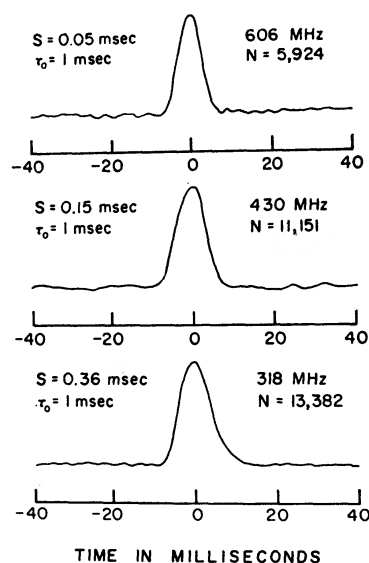


FIG. 4.—Average pulse profiles of JP 1933 at high radio frequencies. The intermediate-frequency bandwidth of 10 kHz caused a dispersion smearing of S , the postdetection RC time constant was τ_0 , and the number of pulses averaged was N . The zero corresponds to the zero time phase when the delay due to dispersion, $\int n_e dl = 158.60 \pm 0.05$ pc cm $^{-3}$, is corrected for.

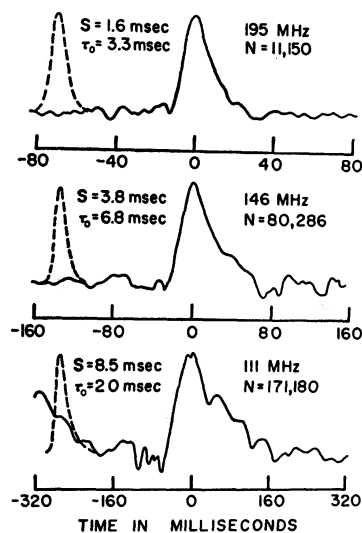


FIG. 5.—Average pulse profiles of JP 1933 at low radio frequencies (*solid lines*). The dashed profile is that profile which would be observed if the pulse profile were independent of frequency. The intermediate-frequency bandwidth of 10 kHz caused a dispersion smearing of S , the postdetection RC time constant was τ_0 , and the number of pulses averaged was N . The zero corresponds to the zero time phase when the delay due to dispersion, $\int n_e dl = 158.60 \pm 0.05$ pc cm $^{-3}$, is corrected for.

sion across the intermediate-frequency bandpass was calculated. This function was then convolved with the observed profile at 606 MHz and with an exponential function whose e^{-1} decay time was f_ν^{-1} . The resulting profiles (Fig. 6) agree well with those observed. Under the assumption that the emitted pulse profile is not a strong function of the radio frequency, the profiles in Figures 4, 5, and 6 indicate that the pulse broadening due to

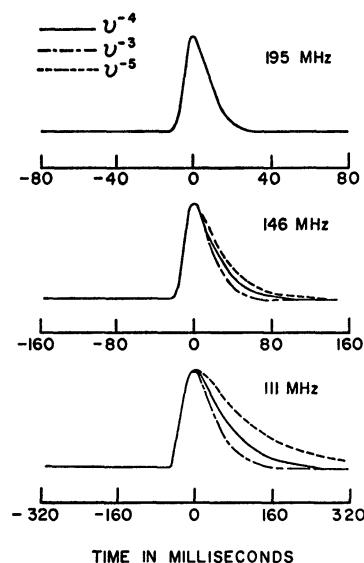


FIG. 6.—Theoretical low-frequency pulse profiles formed by assuming that the pulse broadening caused by interstellar scintillation is equivalent to convolving the high-frequency profile with an exponential function. The e^{-1} decay times of the exponentials were taken to vary with frequency to the minus third, fourth, and fifth power. The profiles include an additional convolution which takes into account the observational parameters given in Fig. 5.

interstellar scintillation is equivalent to a convolution of the emitted profile with an exponential function whose e^{-1} width is f_ν^{-1} . In addition, they show that f_ν^{-1} is proportional to $\nu^{-4.0 \pm 0.7}$ and to the square of the dispersion measure, in agreement with equation (4).

d) Decorrelation Times

An earlier paper (Lang 1969) has shown that three pulsars have decorrelation times τ_ν which vary as $\nu^{+1.0 \pm 0.3}$ as suggested by equation (6). Rickett (1970) has also presented data which indicate that τ_ν is proportional to $\nu^{+0.9 \pm 0.6}$ for several pulsars. Here this consistency with equation (6) is shown to hold over a large range of frequencies and is extended to other pulsars.

Measurements of decorrelation times have been made at 111, 318, and 606 MHz. For the 111- and 318-MHz radio frequencies, pulse intensities were calculated from data simultaneously recorded with radiometers with 10-msec time constants and bandwidths of 50 and 500 kHz. Additional intensities were calculated from data recorded with a radiometer with a 10-msec time constant, a 1-MHz bandwidth, and a radio frequency of 606 MHz. A power spectrum of the fluctuations of the ON intensity about its mean value was taken on an array of 2048 points of intensity by means of the Cooley-Tukey algorithm. Similar spectra taken from the OFF intensities were then subtracted from each ON spectrum. At least nine resultant spectra were then added to give the spectra shown in Figure 7.

Recent papers on interplanetary scintillations (Lovelace *et al.* 1970; Cronyn 1970*b*) have indicated that the relevant power spectra may be power law. Therefore, the spectra in Figure 7 were plotted on a log-log scale. A comparison of the spectra with the Gaussian functions shown in Figure 7 indicate that some of the spectra have a non-Gaussian high-frequency tail which may be power law. In this context, it is interesting to note that power spectra of interplanetary scintillations near the Sun have a non-Gaussian high-frequency tail (Cohen and Gundermann 1969). The power spectra could be power law

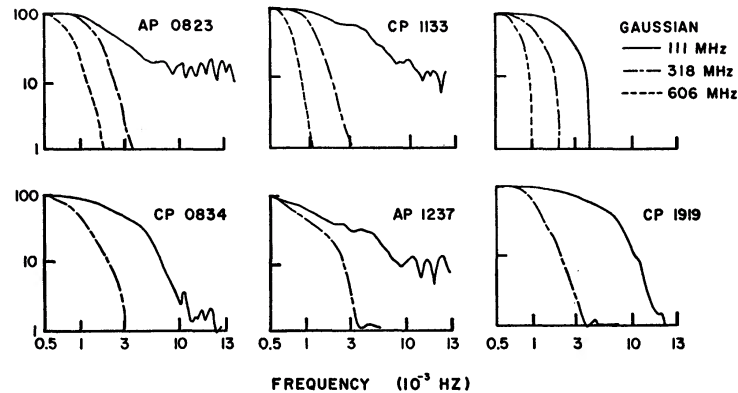


FIG. 7.—The sum of at least nine power spectra of 2048 points of intensity. Pulse intensities were calculated from data simultaneously recorded at 111 and 318 MHz by radiometers with 10-msec time constants and respective bandwidths of 50 and 500 kHz. The 606-MHz intensities were calculated from data recorded by a radiometer with a 10-msec time constant and a 1-MHz bandwidth. Theoretical Gaussian spectra whose full widths at half-maxima are inversely proportional to frequency are also shown.

with a low-frequency roundoff due to Fresnel filtering. It is difficult to distinguish however, between a high-index power-law function and a Gaussian function.

Our main purpose in presenting Figure 7, however, is not to imply any special functional dependence for the power spectra, but to show that any reasonable measurement of the widths of the power spectra gives a width dependence which is proportional to $\nu^{-1.0 \pm 0.5}$. For comparison, Figure 7 also shows theoretical Gaussian spectra whose full widths at half-maximum are proportional to $\nu^{-1.0}$. It is clear that the equivalent widths of the observed spectra go as $\nu^{-1.0 \pm 0.5}$. Consequently, τ_ν , which is the equivalent width of the Fourier transform of these spectra, must be proportional to $\nu^{+1.0 \pm 0.5}$, in agreement with equation (6). Values of τ_{318} given in Table 1 indicate that the dependence of τ_ν on dispersion measure also agrees with equation (6).

e) Modulation Indices and Probability Distributions of Intensity

The relative rms value of the intensity fluctuations about the mean intensity have been calculated for all pulsars which are visible at Arecibo, and which have decorrelation frequencies $\gtrsim 50$ kHz at 111, 318, and 430 MHz. These modulation indices m are defined by

$$m = \{[(\sigma_{\text{on}})^2 - (\sigma_{\text{off}})^2] / [\langle I_{\text{on}}(t) \rangle - \langle I_{\text{off}}(t) \rangle]^2\}^{1/2}. \quad (10)$$

When they were calculated for unsmoothed data, the m had a value of 1.0 ± 0.3 for every source, and m was found to be independent of observing frequency in the interval 111–606 MHz.

In order to ensure that probability distributions would be independent of the pulse-to-pulse variations, which are thought to be intrinsic to the source, trains of pulse intensities were smoothed by running means over twenty-five pulses. After calculating the average intensity of the ON pulses, $\langle I_{\text{on}} \rangle$, frequency histograms were formed by counting the number of times an intensity I fell within the interval $I \pm \langle I_{\text{on}} \rangle / 20.0$ (Fig. 8). In each case the observing bandwidth was narrower than the decorrelation frequency and the time constant was 10 msec. The modulation indices were also calculated and are given in Figure 8, together with the corresponding Rice-squared and lognormal distributions. These modulation indices are slightly less than unity because smoothed data were used. The lognormal distribution is included because that distribution has been suggested as a more appropriate one in recent papers (Tatarski 1961; Ochs and Lawrence 1969; Young

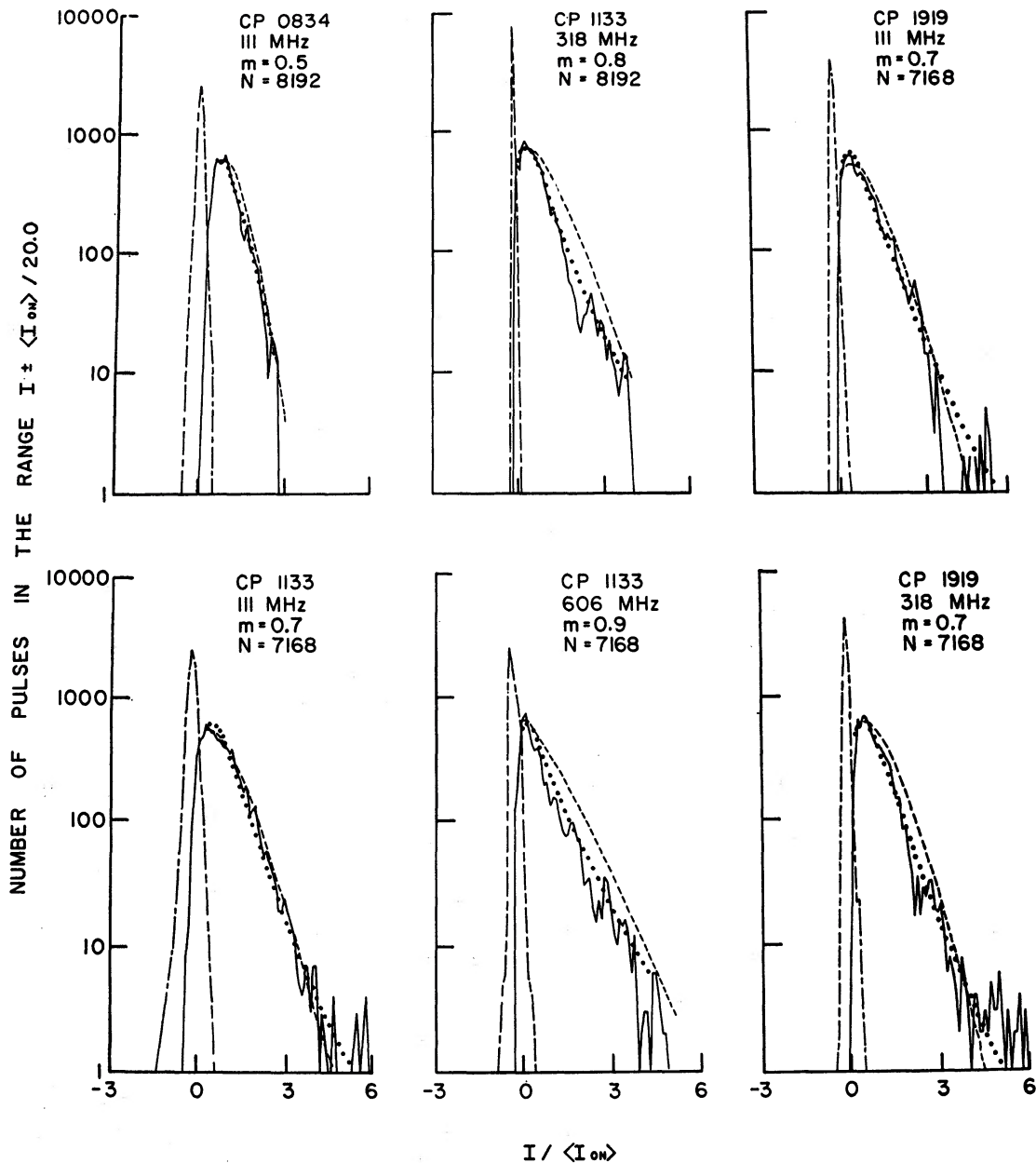


FIG. 8.—Frequency histograms representing probability distributions of pulsar-radiation intensity I . A sequence of N pulses was smoothed by a running mean over 25 pulses before forming the histograms. *Solid lines*, histograms formed from intensities on the pulse; *broken dashed lines*, those formed from intensities off the pulse. The modulation index m was used to calculate theoretical lognormal (*dotted line*) and Rice-squared (*dashed line*) distributions.

1970). Although the ON probability distribution (*solid line*) is actually the convolution of the interstellar probability distribution with the OFF probability distribution (*broken dashed line*), the OFF histogram is sufficiently narrow to indicate that, in most cases, both the Rice-squared and lognormal distributions accurately describe the interstellar medium.

f) *The Scale Size and the Root-Mean-Square Fluctuating Electron Number Density of the Interstellar Medium*

Recent joint observations of CP 1133 between the Arecibo and Jodrell Bank Observatories showed highly correlated intensity fluctuations at 408 MHz with a time delay of 50 pulse periods. These observations (Lang and Rickett 1970) result in the following criteria:

$$5 \times 10^8 \text{ cm} \lesssim \frac{c}{2\pi\nu\theta_{\text{scat}}} < 3 \times 10^9 \text{ cm} \quad (11)$$

for CP 1133 at 408 MHz.

If we choose $\frac{1}{2}c/\pi\nu\theta_{\text{scat}} = 10^9 \text{ cm}$, then $\theta_{\text{scat}} \approx 2 \times 10^{-3}$ seconds of arc. Using this value of θ_{scat} and $f_{408} \approx 10^6 \text{ Hz}$ in equation (3), we obtain $D \approx 300 \text{ pc}$ for CP 1133. Equation (7) then leads to the following limits:

$$10^9 \text{ cm} < a < 10^{12} \text{ cm} . \quad (12)$$

Using $\theta_{\text{scat}} \approx 2 \times 10^{-3}$ seconds of arc, $a \approx 10^{11} \text{ cm}$, and $D \approx 300 \text{ pc}$ in equation (2), we obtain $\langle \Delta n_e^2 \rangle^{1/2} \approx 3 \times 10^{-4} \text{ cm}^{-3}$.

In view of the work of Tatarski (1961), Jokipii and Hollweg (1970), and Lovelace *et al.* (1970), it is interesting to note that a is roughly the first Fresnel zone in size, $a \approx (cD/2\nu)^{1/2} \approx 10^{11} \text{ cm}$. These authors suggest that the a inferred from scintillation arguments may be limited in size to the first Fresnel zone, rather than actually being a measure of the scale of the fluctuations in electron density. If the similarity of the observed a and the size of the Fresnel zone is not a coincidence, then the scale of the density irregularities may be much larger than that inferred from the observed intensity fluctuations. Evidence against the supposition that the irregularities are larger is provided, however, by the fact that f_ν does not vary faster than ν^4 .

The parameter θ_{scat} , however, is related to f_ν and D by equation (3) which follows from simple geometrical arguments. Consequently, the use of measured values of f_ν together with known dispersion measures and reasonable estimates of $\langle n_e \rangle$ gives estimates of θ_{scat} which follow even if a is not the actual size of the electron-density fluctuations. In fact, most of the conclusions given in the next section (those regarding the angular sizes of pulsars, the relative velocities of the pulsars and/or the interstellar medium with respect to the Earth, the minimum detectable period of a pulsar, and the minimum detectable size of a radio source) follow from geometrical arguments which relate observed data and which are independent of the true character of a .

g) *The Critical Frequency for Weak Scintillations*

In § III f we specified $a \approx 2 \times 10^{11} \text{ cm}$ and $\langle \Delta n_e^2 \rangle^{1/2} \approx 3 \times 10^{-4} \text{ cm}^{-3}$ for CP 1133 which has $D \approx 300 \text{ pc}$. At this distance, and with these values of a and $\langle \Delta n_e^2 \rangle^{1/2}$, equation (8) indicates that interstellar scintillation will become weak for frequencies higher than $\nu_c \approx 2 \times 10^9 \text{ Hz}$. Weak scattering will be observed at lower frequencies for nearer pulsars and at higher frequencies for more distant ones.

Downs and Reichley (1970) have recently provided independent confirmation of these values of a , $\langle \Delta n_e^2 \rangle^{1/2}$, and ν_c , and of the thin-screen model, by observing pulsar-scintillation parameters at 2388 MHz. They find that the two nearby pulsars, CP 0950 with $D \approx 180 \text{ pc}$ and CP 1133 with $D \approx 300 \text{ pc}$, exhibit a decorrelation time which is the same as that at nearby lower frequencies, have respective modulation indices m of 0.14 and 0.45, and have nearly Gaussian distributions of intensity. In addition, they find that five more distant pulsars still exhibit the expected strong scattering with decorrelation times $\tau_\nu \propto \nu$, $m \approx 1.0$, and nearly exponential probability distributions. Their data are too noisy to distinguish between the exponential, Rice-squared, and lognormal distributions shown in Figure 8.

IV. PARAMETERS OF THE PULSARS AND THE INTERSTELLAR MEDIUM

a) *Pulsar Distances and the Average Number Density of Electrons*

Typical scale sizes $a \approx 10^{11}$ cm and rms fluctuating electron number densities $\langle \Delta n_e^2 \rangle^{1/2} \approx 3 \times 10^{-4} \text{ cm}^{-3}$ (cf. § III f) can be used with measured values of the decorrelation frequencies f , to obtain pulsar distances D from equation (3). These distances, which are given in Table 1, assume an isotropic, homogeneous distribution of fluctuating electrons. Consequently, the distance estimates may be in error for distances larger than a few hundred parsecs. It is noted, however, that our distance estimate of the Crab pulsar NP 0532 is $D \approx 2220$ pc, which is in agreement with other distance estimates to the Crab Nebula (Trimble 1968).

Once the distance D has been obtained, it may be used with the dispersion measures to obtain an estimate of the average number density $\langle n_e \rangle$ of electrons along the line of sight to the pulsar. These densities, which are also given in Table 1, have the average value of 0.032 cm^{-3} . As Davidson and Terzian (1969) have pointed out, this value of $\langle n_e \rangle$ is consistent with low-frequency absorption measurements if we assume that the electrons are concentrated in clouds filling 10 percent of space, and having internal electron densities of the order of 0.3 cm^{-3} . In this case, $\langle n_e^2 \rangle^{1/2} = 0.1 \text{ cm}^{-3}$ and the electron temperature is $T_e \approx 5000^\circ \text{ K}$.

b) *Angular Sizes of Pulsars*

Assuming that an average pulsar is at a distance $D \approx 500$ pc, we may use $a \approx 10^{11}$ cm and $\langle \Delta n_e^2 \rangle^{1/2} \approx 3 \times 10^{-4} \text{ cm}^{-3}$ in equation (5) to obtain the critical angle $\psi_c \approx 10^{-7}$ seconds of arc. The pulsar must be smaller than 10^{-7} seconds of arc in order for an Earth observer to detect fluctuations in intensity caused by interstellar scintillation. At a distance of 100 pc, this angular size corresponds to a physical size of 1000 km. The conclusion that pulsars must be smaller than 1000 km in diameter is not surprising, as the same criterion can be deduced from normal pulse widths of ≈ 30 msec and the usual light-time argument. The scintillation-width measurement, however, does not depend on the isotropy of the source, whereas the light-time argument does. In addition, it is important to note that 10^{-7} seconds of arc is considerably smaller than the angular size of any observable self-absorbed synchrotron radio source (cf. Sligh 1963; Kellermann and Pauliny-Toth 1969). Conventional radio sources will not exhibit observable intensity fluctuations caused by interstellar scintillation.

c) *Relative Velocities of the Pulsars and/or the Interstellar Medium with Respect to the Earth*

Assuming $\tau_{318} \approx 10^3$ sec, $D \approx 300$ pc, $a \approx 10^{11}$ cm, and $\langle \Delta n_e^2 \rangle^{1/2} \approx 3 \times 10^{-4} \text{ cm}^{-3}$, we obtain the velocity $v \approx 50 \text{ km sec}^{-1}$ from equation (6). Observed values of τ , and D allow a velocity range of 30–200 km sec^{-1} for the pulsars. Although these measurements may be taken to indicate that pulsars do not have velocities on the order of several thousand km sec^{-1} , they do not exclude the possibility that pulsars may be “runaway” stars with velocities on the order of 100 km sec^{-1} (cf. Prentice 1970; Gott, Gunn, and Ostriker 1970). It is also noted that the observed velocities have the same order of magnitude as the velocity of the Earth with respect to the Sun, $\approx 30 \text{ km sec}^{-1}$, and the velocity of the Sun with respect to the local group of stars, $\approx 20 \text{ km sec}^{-1}$.

d) *Minimum Detectable Period of a Pulsar*

Nearby observed pulsars exhibit a pulse broadening of about 5 msec which is just detectable as a trailing elongation of pulses at 40 MHz (Craft 1970). As reported in § III c, more distant pulsars exhibit a broadening of tens of milliseconds in the observable radiofrequency range. Such broadening will prohibit the detection of distant fast pulsars with periods smaller than a few milliseconds. These pulsars might be observed, however,

at very high radio frequencies or at optical frequencies where the interstellar-scintillation effects are no longer present. In this context, it is interesting to note that the fastest observed pulsar has a period of 33 msec. The absence of observed short-period pulsars could be due to scintillation effects or to the short lifetime of fast pulsars.

e) Minimum Detectable Angular Size of a Radio Source

As shown in § III *f*, the rms scattering angle $\theta_{\text{scat}} \approx 10^{-3}$ seconds of arc at 318 MHz for a source at a distance of 300 pc. This minimum detectable size for a radio source may be taken to be proportional to $(\int n_e^2 dl)^{1/2}$ and inversely proportional to the square of the observing frequency. Interplanetary scintillations or long-baseline interferometry of radio sources at low radio frequencies may permit measurements of θ_{scat} and the $(\int n_e^2 dl)^{1/2}$ for various lines of sight through the Galaxy. As Harris, Zeissig, and Lovelace (1970) have pointed out, such observations must be made at low radio frequencies and for weak radio sources in order to make θ_{scat} larger than the angular size due to synchrotron self-absorption.

Throughout this discussion we have assumed that the interstellar medium is homogeneous and isotropic, that $\langle \Delta n_e^2 \rangle^{1/2}$ is proportional to $\langle n_e \rangle$, and that refraction effects are negligible. Anisotropies, variations in the ratio $\langle \Delta n_e^2 \rangle^{1/2} / \langle n_e \rangle$, and refraction effects may cause θ_{scat} and f_ν^{-1} to vary from the predicted values. As an example of this, Ables, Komesaroff, and Hamilton (1970) have recently measured $\theta_{\text{scat}} \approx 0.1$ arc sec and $f_\nu^{-1} \approx 4$ msec for PSR 0833-45 at 408 MHz. These abnormally high values may be attributed to the Gum Nebula (Gum 1955) which lies about half way between the pulsar and the solar system. Very long-baseline interferometry might be expected to detect similar differences between the general predictions specified in this paper and the properties of interstellar matter along specific lines of sight through the Galaxy.

Many authors (Burbidge and Hoyle 1969; Matvienko 1969; Drake 1970; Cronyn 1970*a*; Rankin *et al.* 1970) have suggested that the compact source in the Crab Nebula is the pulsar NP 0532. Several of these authors argue that the pulsar becomes a continuum source at low frequencies due to pulse broadening by scintillation. Although the point will not be belabored here, it will be shown that such a point of view is consistent with the general properties of interstellar scintillation. In particular, by using $\nu = 26$ MHz, $D = 2000$ pc, $a \approx 10^{11}$ cm, and $\langle \Delta n_e^2 \rangle^{1/2} \approx 3 \times 10^{-4}$ cm⁻³ in equation (2), we obtain $\theta_{\text{scat}} \approx 1''$. This is the angular size of the compact source in the Crab Nebula at 26 MHz (Cronyn 1970*a*). Cronyn (1970*c*) has also shown that the angular size of the compact source is proportional to ν^{-2} , which is suggested by equation (2) for θ_{scat} . It is noted, however, that these scattering measurements are inconsistent with the view that the pulse broadening is caused by a scattering atmosphere near the pulsar (cf. Code 1970).

V. CONCLUSIONS

It is concluded that a model in which a phase screen of thickness D is located along the line of sight at a distance $\frac{1}{2}D$, half the Earth-pulsar distance, adequately describes the observable characteristic parameters of pulsar long-term variations in intensity. In particular, we note the following:

a) Decorrelation frequencies are proportional to the fourth power of the observing frequency and inversely proportional to the square of the dispersion measure.

b) Pulse broadening is equivalent to convolving the emitted pulse profile with an exponential function whose e^{-1} decay time is proportional to the square of the dispersion measure and inversely proportional to the fourth power of the observing frequency.

c) Decorrelation times are proportional to the observing frequency and weakly dependent on dispersion measure. Power spectra of intensity fluctuations are nearly Gaussian in form, but have a non-Gaussian, high-frequency tail which may be power law.

d) Modulation indices are nearly unity and are independent of observing frequency in the interval 111–606 MHz. Both Rice-squared and lognormal probability distribution functions fit the observed probability distributions of intensity well.

e) The scale size a is $\approx 10^{11}$ cm, which is roughly the first Fresnel zone in size. The rms value of the fluctuating electron number density, $\langle \Delta n_e^2 \rangle^{1/2}$, has the value of 3×10^{-4} cm $^{-3}$.

f) Pulsar scintillations will become weak at frequencies above 2000 MHz for nearby pulsars; and this phenomenon has been observed.

The substantial agreement of observed statistical quantities with the model allows the following to be confidently specified:

a) Pulsar distances are calculated and used with dispersion measures to measure the average number density of electrons along the line of sight to the pulsars, $\langle n_e \rangle \approx 0.03$ cm $^{-3}$.

b) Pulsars are smaller than 10^{-7} seconds of arc. Observable self-absorbed synchrotron radio sources will not give rise to observable intensity fluctuations caused by interstellar scintillation.

c) The relative velocities of the pulsars and/or the interstellar medium with respect to the Earth lie in the range 30–200 km sec $^{-1}$.

d) Pulsars with periods smaller than a few milliseconds will not be detected at frequencies below a few hundred MHz, but may be detected at higher radio frequencies or at optical frequencies.

e) The minimum detectable size of a radio source at a distance of 300 pc will be on the order of 10^{-3} seconds of arc at 318 MHz. This size is proportional to $(\int n_e^2 dl)^{1/2}$ and inversely proportional to the square of the observing frequency. Interplanetary scintillation or very long-baseline interferometry of radio sources at low radio frequencies may provide a measurement of the $(\int n_e^2 dl)^{1/2}$ along various lines of sight through the Galaxy.

f) The compact source of the Crab Nebula is almost certainly the pulsar NP 0532. The pulsar becomes a continuum source at low radio frequencies due to the pulse broadening caused by interstellar scattering.

The author is grateful for discussion and/or communications with M. H. Cohen, J. M. Comella, H. D. Craft, W. M. Cronyn, G. S. Downs, F. D. Drake, A. Hewish, C. E. Heiles, R. V. E. Lovelace, J. M. Rankin, P. E. Reichley, J. A. Roberts, E. E. Salpeter, D. H. Staelin, A. T. Young, and G. A. Zeissig. The Arecibo Observatory is operated by Cornell University under contract to the National Science Foundation and with partial support from the Advanced Research Projects Agency. This work was supported in part by the Air Force Office of Scientific Research, Office of Aerospace Research, U.S. Air Force, under contract F44620-69-C-0092.

REFERENCES

- Ables, J. G., Komesaroff, M. M., and Hamilton, P. A. 1970, *Ap. Letters*, **6**, 147.
 Burbidge, G., and Hoyle, F. 1969, *Nature*, **221**, 847.
 Code, A. D. 1970, *Ap. J. (Letters)*, **159**, L29.
 Cohen, M. H., and Gundermann, E. J. 1969, *Ap. J.*, **155**, 645.
 Cohen, M. H., Gundermann, E. J., Hardebeck, H. E., and Sharp, L. E. 1967, *Ap. J.*, **147**, 449.
 Craft, H. D., Jr. 1970, Ph.D. thesis, Department of Astronomy and Space Sciences, Cornell University, *CRSR Rept.* 395.
 Cronyn, W. M. 1970a, *Science*, **168**, 1453.
 ———. 1970b, *Ap. J.*, **161**, 755.
 ———. 1970c, unpublished Ph.D. thesis, University of Maryland
 Davidson, K., and Terzian, Y. 1969, *A.J.*, **74**, 849.
 Downs, G. S., and Reichley, P. E. 1970, paper presented at the Spring 1970 meeting of URSI.
 Drake, F. D. 1970, *Pub. A.S.P.*, **82**, 486.
 Ewing, M. S., Batchelor, R. A., Staelin, D. H., and Friefeld, R. D. 1970, talk presented at the 132nd meeting of the A.A.S.

- Fejer, J. A. 1953, *Proc. R. Soc. London, A*, **220**, 455.
 Gott, J. R., Gunn, J. E., and Ostriker, J. P. 1970, *Ap. J. (Letters)*, **160**, L91.
 Gum, C. S. 1955, *Mem. R.A.S.*, **67**, 155.
 Harris, D. E., Zeissig, G. A., and Lovelace, R. V. 1970, *Astr. and Ap.*, **8**, 98.
 Huguenin, G. R., Taylor, J. H., and Jura, M. 1969, *Ap. Letters*, **4**, 71.
 Jokipii, J. R., and Hollweg, J. V. 1970, *Ap. J.*, **160**, 745.
 Kellermann, K. I., and Pauliny-Toth, I. I. K. 1969, *Ap. J. (Letters)*, **155**, L71.
 Komesaroff, M. M., McCulloch, P. M., Hamilton, P. A., and Cooke, D. J. 1968, *Nature*, **220**, 358.
 Lang, K. R. 1969, *Science*, **166**, 1401.
 Lang, K. R., and Rickett, B. J. 1970, *Nature*, **225**, 528.
 Lovelace, R. V. E., Salpeter, E. E., Sharp, L. E., and Harris, D. E. 1970, *Ap. J.*, **159**, 1047.
 Matvienko, L. E. 1969, Lebedev Institute Circular.
 Mercier, R. P. 1962, *Proc. R. Soc. London, A*, **58**, 382.
 Ochs, G. R., and Lawrence, R. S. 1969, *J. Opt. Soc. Am.*, **59**, 226.
 Prentice, A. J. R. 1970, *Nature*, **225**, 438.
 Rankin, J. M., Comella, J. M., Craft, H. D., Jr., Richards, D. W., Campbell, D. B., and Counselman, C. C., III. 1970, *Ap. J.*, **162**, 707.
 Rickett, B. J. 1969, *Nature*, **221**, 158.
 ———. 1970, *M.N.R.A.S.*, **150**, 67.
 Salpeter, E. E. 1967, *Ap. J.*, **147**, 433.
 ———. 1969, *Nature*, **221**, 31.
 Scheuer, P. A. G. 1968, *Nature*, **218**, 920.
 Scott, P. F., and Collins, R. A. 1968, *Nature*, **218**, 230.
 Slish, V. I. 1963, *Nature*, **199**, 682.
 Staelin, D. H., and Reifenstein, E. C. 1969, *Ap. J. (Letters)*, **156**, 121.
 Staelin, D. H., and Sutton, J. M. 1970, *Nature*, **226**, 69.
 Tatarski, V. I. 1961, *Wave Propagation in a Turbulent Medium* (New York: McGraw-Hill Book Co.).
 Trimble, V. 1968, *A.J.*, **73**, 535.
 Uscinski, B. J. 1968a, *Phil. Trans., Roy. Soc. London A262*, 609.
 ———. 1968b, *Proc. R. Soc. London, A*, **307**, 471.
 Vitkevich, V. V. and Shitov, Y. P. 1970, *Nature*, **226**, 1235.
 Young, A. T. 1970, submitted to *M.N.R.A.S.*